Chemistry–A European Journal
Research Article
doi.org/10.1002/chem.202201527
Chemistry Europe
European Chemical Societies Publishing
www.chemeurj.org

[2+3] Amide Cages by Oxidation of [2+3] Imine Cages – Revisiting Molecular Hosts for Highly Efficient Nitrate Binding

Jochen C. Lauer,[a] Avinash S. Bhat,[a] Chantal Barwig,[a] Nathalie Fritz,[a] Tobias Kirschbaum,[a] Frank Rominger,[a] and Michael Mastalerz*[a]

Abstract: The pollution of groundwater with nitrate is a serious issue because nitrate can cause several diseases such as methemoglobinemia or cancer. Therefore, selective removal of nitrate by efficient binding to supramolecular hosts is highly desired. Here we describe how to make [2+3] amide cages in very high to quantitative yields by applying an optimized Pinnick oxidation protocol for the conversion of corresponding imine cages. By NMR titration experiments of the eight different [2+3] amide cages with nitrate, chloride and hydrogen sulfate we identified one cage with an unprecedented high selectivity towards nitrate binding vs. chloride ($S=705$) or hydrogensulfate ($S>13500$) in CD_2Cl_2/CD_3CN (1:3). NMR experiments as well as single-crystal structure comparison of host-guest complexes give insight into structure-property-relationships.

Introduction

Shape-persistent organic cages are attractive synthetic targets, due to their defined cavities, which can be tailored in size, geometry and with diverse functional groups.[1][2] This allows to precisely provide defined molecules for selective binding or recognition of molecules and ions, either in the solid state (e.g. for gas sorption,[3] as stationary phase for chromatography,[4] or deposited on surfaces such as on quartz crystal microbalances for gravimetric sensing of airborne vapors,[5] or in solution to perform 'classical' host-guest recognition by NMR or UV-Vis-titration or isothermal calorimetry.[6]

The structural design of host molecules suitable for selective anion binding or recognition is still ongoing, although this topic has been of interest to supramolecular chemists for some time.[7] Especially smaller charge-neutral cages regained some attention recently due to their high selectivity and association constants (K_a's) for anion binding.[8] For instance, Flood and coworkers introduced the triazole-based organic cage **1** (Figure 1) that was able to bind chloride ions with attomolar affinity ($K_a=10^{17}$ M^{-1}).[9] Badjic and coworkers presented the hexapodal capsule **2**, which was studied for anion recognition,[10] finding a clear preference for tetrahedral oxo-anions, such as sulfate and hydrogenphosphate, rather than binding halides or carbonate. Other shape-persistent organic cages have been designed for example to selectively bind to tetrahedral anions,[11] or even used to undergo anion-π catalysis.[12] In the past, TREN-based C_3-symmetric amide cages (**3**; so called Bowman-James cages) have been shown to be superior hosts for anion recognition with a preference for halides, such as chloride or fluoride.[13] A structurally comparable cage **4** was described by Anslyn and coworkers in 1997, reporting a good selectivity ($S=7.5$) for nitrate vs. halides ($K_a(NO_3^-)=300$ M^{-1} and $K_a(Cl^-)=40$ M^{-1}).[14]

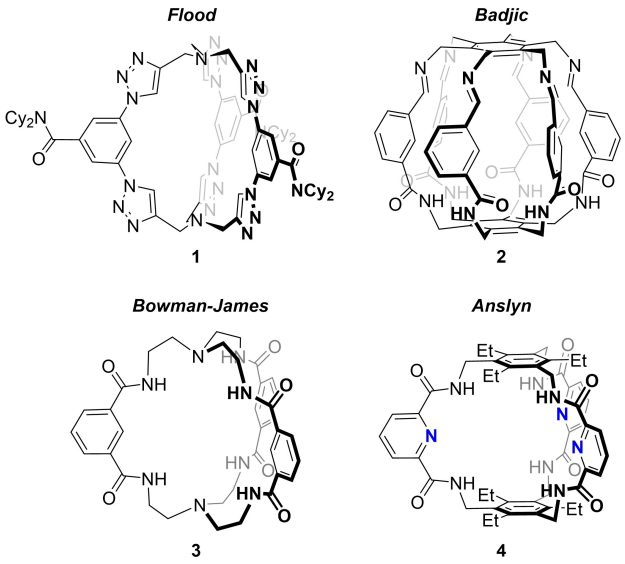

Figure 1. Examples of cages for anion recognition from literature.[9,10,13b,14]

[a] J. C. Lauer, Dr. A. S. Bhat, C. Barwig, N. Fritz, T. Kirschbaum, Dr. F. Rominger, Prof. Dr. M. Mastalerz
Organisch-Chemisches Institut
Ruprecht-Karls-Universität Heidelberg
Im Neuenheimer Feld 270, 69120 Heidelberg (Germany)
E-mail: michael.mastalerz@oci.uni-heidelberg.de

Supporting information for this article is available on the WWW under https://doi.org/10.1002/chem.202201527

Nitrate pollution in groundwater became a critical issue,[15] and nitrate concentrations of >50 mg/L are according to the World Health Organization (WHO) causing serious health risks for humans (for example, colorectal cancer, bladder cancer, breast cancer, thyroid disease and infant methemoglobinemia).[16] Therefore, the construction of a highly selective nitrate binding host is desired to for example remove it from drinking water.[17] However designing synthetic receptors suitable for selective recognition of nitrate is challenging due to the anion's low hydrogen bonding affinity and high energy of solvation.[18]

A closer look to Anslyn's tripodal receptor cage **4** reveals that the distance of the two π-faces of the bottom and top benzene units is about 7.0 Å, which is exactly two times the ideal distance of π-stacking and that hosted nitrate (which is a trigonal planar molecule with π-surfaces itself) can be modeled to be sandwiched parallel between those two aromatic units. By changing the electronic contributions of the three substituents of those aromatic units, the contribution of π-stacking to the affinity of nitrate to the binding pocket should be adjustable. This is different to all other cages depicted in Figure 1, where such a fine-tuning is not possible and to our surprise has not been explored yet for cage **4**. In this respect, it is worth to be mentioned that the influence of electronic demand in an aryl-based C_3-symmetric tris-urea for anion recognition was studied.[17h] Although by NMR titration experiments a clear difference of association constants (K_a) for 1:1 complexes with nitrate were found in dependency of the substituents of the central aryl rings (F or H), with a preference for the F-substituted one ($K_{a,F}=24100\ M^{-1}$ vs. $K_{a,H}=11800\ M^{-1}$), the crystal structures of nitrate complexes gave a different picture with two nitrate anions bound to one tripodal host molecule (2:1 stoichiometry). One nitrate anion is relatively close to the central benzene ring suggesting at least some type of π-stacking although it is not ideally parallel oriented.

The second possibility to fine-tune the cage towards nitrate binding is to adjust the strength of the hydrogen-bonding donation ability of the amide units. Anslyn's cage **4** contains pyridine linkers, which on one hand withdraws electron density of the amide bonds and make them in principle better hydrogen-bonding donors. On the other hand, amide hydrogen's are intramolecular interacting with the pyridine's nitrogen lone pair, reducing their ability to bind to the nitrate anion.[19] Furthermore, the nitrogen lone pair electrons should decrease binding affinity by repulsion of the negatively charge anions.[20] Thus Anslyn's cage **4** has two sites of possible fine-tuning affinities for anion recognition which is described herein.

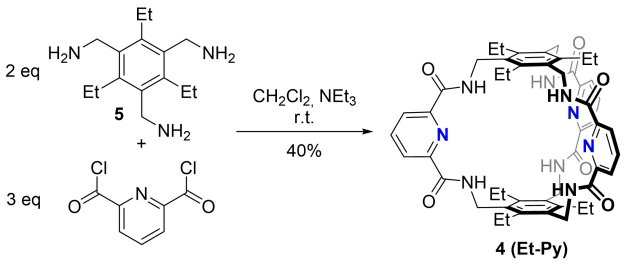

Scheme 1. Amide cage formation done by Anslyn and coworkers.[14]

Results and Discussion

Anslyn's cage **4** (which we name here also **Et-Py**; Et for the ethyl substituents on bottom and top benzene rings and **Py** for the bridging pyridine rings) was originally synthesized by a six-fold amide bond formation of triamine **5** with 2,6-pyridine dicarbonyl dichloride in 40% yield (Scheme 1). Since the cage is synthesized by an irreversible bond formation, the reported yield is according to the authors *"surprisingly high"* and explained by the preorganization of building blocks.[14] Recently, we presented the post-synthetic transformation of [4+6] imine cages to the corresponding amide cages by a twelve-fold Pinnick oxidation.[21] We were interested if this method is applicable to synthesize smaller [2+3] amide cages from the corresponding [2+3] imine cages, which itself usually form in up to quantitative yields.[22]

The Pinnick reaction is based on chloric acid ($HClO_2$), which is formed in situ from $NaClO_2$ in an aqueous acidic medium, that is usually kept pH-stable with NaH_2PO_4 as buffer.[23] Furthermore, a scavenger for generated hypochloric acid (HClO) is added. First, we tested the reaction conditions we applied for the [4+6] imine cages[21] also for the [2+3] imine cage **6**, which was performed in THF and water as solvents, NaH_2PO_4 and $NaClO_2$ as well as an excess (100 equiv.) of 2-methyl-butene as scavenger. After running the reaction for 16 h at room temperature **Et-Ph** cage was isolated in 26% yield (Entry 1, Table 1). Changing the scavenger to H_2O_2 gave basically the same yield (28% Entry 2), although tedious removal of aliphatic by-products deriving from the scavenging reaction was not necessary. By switching the acid from NaH_2PO_4 to acetic acid, keeping H_2O_2 as scavenger, the isolated yield for **Et-Ph** was still in a comparable range (28%, Entry 3). Since the Pinnick oxidation is a relative slow reaction,[23d,24] for cages with multiple imine bonds it competes with acid mediated imine bond

Table 1. Optimization of the Pinnick oxidation of imine cage **6** to **Et-Ph** (see Scheme 2).

Entry	Acid	Solvent	Scavenger	T [°C]	t	Isolated yield
1	NaH_2PO_4	THF/H_2O	2-methyl-2-butene	r.t.	16 h	26%
2	NaH_2PO_4	THF/H_2O	H_2O_2	r.t.	16 h	28%
3	AcOH	THF/H_2O	H_2O_2	r.t.	16 h	28%
4	NaH_2PO_4	THF_{abs}	2-methyl-2-butene	80	7 d	95%
5	NaH_2PO_4	THF_{abs}	α-pinene	80	7 d	95%
6	NaH_2PO_4	1,4-dioxane	2-methyl-2-butene	100	3 d	95%
7	NaH_2PO_4	1,4-dioxane	α-pinene	100	3 d	92%

cleavage,[21,22d,25] if performed in aqueous solution (Entries 1–3). Therefore, water-free conditions were investigated. Running the reaction in THF_{abs}, NaH_2PO_4, $NaClO_2$ and 2-methyl-butene at 80 °C in a closed screw-capped vial for 7 days gave analytically pure cage **Et-Ph** in 95% yield (Entry 4). The relative long reaction times needed are most likely due to the low solubility of the inorganic salts in THF_{abs}. Unfortunately, the used scavenger 2-methyl-2-butene has a low boiling point of 38 °C, making the reaction at this temperature in a closed screw-capped vessel a potential safety hazard. Therefore, α-pinene (bp. 155 °C) was used as scavenger to avoid the evolution of high pressure giving the cage **Et-Ph** in the same yield (95%, Entry 5). Using 1,4-dioxane as solvent at slightly elevated temperatures (100 °C) halved the reaction time to 3 days without loss of yield (95%, Entry 6). Using α-pinene as scavenger in combination with dioxane gives the cage **Et-Ph** in 92% yield (Entry 7). We decided to use the conditions from Entry 5 for the synthesis of further amide cages, as these conditions represent the lowest safety hazard at high yields and at the same time milder conditions.

Applying the optimized conditions to imine cages **7**–**13** gave the corresponding amide cages in yields between 33% and 95% (Scheme 2 and Table 2) and the reaction can be easily scaled up to 1 gram, as has been demonstrated for cage **Et-Ph** (see Supporting Information). Due to the low solubility of the brominated imine cage **12** in THF the conversion to **Br-Ph** was very low. Even with increased reaction times to 14 days a significant amount of incompletely oxidized by-products was found after workup by ^{1}H NMR and MS experiments of the crude material (see Supporting Information, Figure S96). These structurally similar but incompletely converted products were separated by thermal recrystallization from hot DMSO, giving a comparably low yield of 33% due to losses during this purification step. However, with the exception of **Br-Ph** and **F-Py** yields are very high for all other amide cages (up to 95%) showing the advantage of this two-step strategy over a one-step irreversible reaction (40%, one step)[14] and the potential of the general strategy to first construct larger molecules by DCC reactions in high yields and then chemically transform labile bonds to stable bonds to achieve even compounds that are very difficult or even impossible to be synthesized by irreversible bond formations.[21,22e,25a,26] All new cages have been fully characterized including single crystal structure analysis by X-ray diffraction (for details, see Supporting Information).

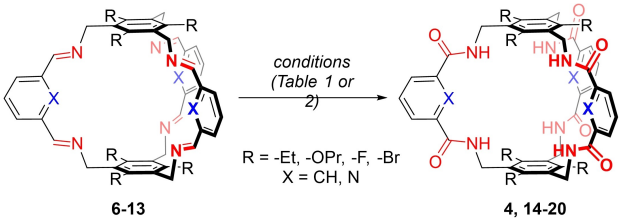

Scheme 2. Pinnick oxidation of [2 + 3] imine cages **6**–**13** to the corresponding amide cages **4**, **14**–**20**. For conditions and yields, see Tables 1 & 2.

The amide cages were studied as potential hosts for binding anions, with a focus on nitrate, but chloride and hydrogen sulfate were also investigated. Therefore, association constants K_a were determined by ^{1}H NMR titration experiments with tetrabutylammonium salts in CD_2Cl_2/CD_3CN (1:3) for the ethyl and propoxyl-substituted cages and in pyridine-d5 for the halogen containing ones (Table 3; for details, see Supporting Information). For Anslyn's cage **Et-Py** we found a comparable association constant of $K_a(NO_3^-) = 2.88 \times 10^2\ M^{-1}$ as reported in the original paper ($K_a(NO_3^-) = 3 \times 10^2\ M^{-1}$), when treated as a 1:1-complex.[14] However, since our job plot showed evidence of the existence of a 1:2 complex (one host and two guests = H_1G_2), we re-examined the results in this direction and found $K_{a(11)}(NO_3^-) = 2.3 \times 10^2\ M^{-1}$ and a comparably small $K_{a(12)}(NO_3^-)$ of $3 \times 10^0\ M^{-1}$, justifying that a binding event of a second nitrate anion can be neglected. Binding of chloride was in the original paper also treated as a 1:1-complex with $K_a(Cl^-) = 4 \times 10^1\ M^{-1}$, even though in the solid state a 1:2 stoichiometry was found. By carefully studying our titration experiments we found clear hints (Jurczak's residual analysis[27] and Job plot), that the system can also be described as a 1:2 system with $K_{a(11)}(Cl^-) = 1.3 \times 10^2\ M^{-1}$ and $K_{a(12)}(Cl^-) = 9\ M^{-1}$, which is in agreement with their crystal structure. The uptake for hydrogen sulfate was negligible ($K_a(HSO_4^-) < 1\ M^{-1}$); similar as found by Anslyn and coworkers before ($K_a(HSO_4^-) < 5\ M^{-1}$).

By exchanging the pyridyl units by phenyl units (**Et-Ph**), association constants increased about one order of magnitude for nitrate ($K_a(NO_3^-) = 6.8 \times 10^3\ M^{-1}$) and two orders of magnitude for chloride ($K_{a(11)}(Cl^-) = 2.2 \times 10^4\ M^{-1}$, $K_{a(12)}(Cl^-) = 1.54 \times 10^2\ M^{-1}$) – again we found a H_1G_2-system for the binding of chloride with a comparable small $K_{a(12)}$ vs. a two magnitudes higher $K_{a(11)}$. For hydrogensulfate, the affinity increased significantly. We observed an H_2G_1 complex ($K_{a(21)}(HSO_4^-) = 5.7 \times 10^3\ M^{-1}$) present at low concentrations, whereas at higher

Table 2. Yields of the amide cage screening using the conditions from Table 1, Entry 5.

Imine	Amide	R	X	*t*	Yield [%]	Overall[a] Yield [%]
6	**Et-Ph (14)**	Et	CH	7 d	95	95
7	**Et-Py (4)**	Et	N	3 d	95	85–88
8	**OPr-Py (15)**	OPr	N	3 d	90	83
9	**OPr-Ph (16)**	OPr	CH	7 d	87	71
10	**F-Py (17)**	F	N	3 d	48	9.6
11	**F-Ph (18)**	F	CH	5 d	84	37
12	**Br-Py (19)**	Br	N	5 d	90	81
13	**Br-Ph (20)**	Br	CH	14 d	33	14

[a] Yield over two steps, including the imine cage formation.

Table 3. Comparison of NMR titration results. K_{11} represents the association constant of the H_1G_1 complex, K_{12} of the H_1G_2 complex and K_{21} of the H_2G_1 complex.

Entry	Compound	Solvent	K_a (NO_3^-)/[M^{-1}][a]	K_a (Cl^-)/[M^{-1}][a]	K_a (HSO_4^-)/[M^{-1}][a]	S (NO_3^-/Cl^-)[c]	S (NO_3^-/HSO_4^-)[c]
1	**Et-Py**	CD_2Cl_2/CD_3CN (1:3)	$K_{11}(2.3\pm0.3)\times10^2$ $K_{12}(3\pm1)\times10^0$	$K_{11}(1.3\pm0.3)\times10^2$ $K_{12}(9\pm2)\times10^0$	<1	1.77	>230
2	**Et-Py**	pyridine-d5	$K_{11}(2.77\pm0.07)\times10^3$ $K_{12}(6\pm3)\times10^1$	$K_{11}(1.9\pm0.3)\times10^3$ $K_{12}(1.4\pm0.2)\times10^2$	$(5.9\pm0.6)\times10^1$[b]	1.46	47
3	**Et-Ph**	CD_2Cl_2/CD_3CN (1:3)	$(6.8\pm0.1)\times10^3$	$K_{11}(2.2\pm0.1)\times10^4$ $K_{12}(1.54\pm0.05)\times10^2$	$K_{21}(5.7\pm0.2)\times10^3$ $K_{11}>10^5$	0.31	$\ll1$
4	**Br-Py**	pyridine-d5	$(9.1\pm0.2)\times10^3$	$K_{11}(7.0\pm0.2)\times10^3$ $K_{12}(4.8\pm0.2)\times10^1$	$K_{21}(7\pm1)\times10^4$ $K_{11}(4.2\pm0.8)\times10^3$	1.3	0.13
5	**Br-Ph**	pyridine-d5	$>10^5$	$K_{11}>10^5$ $K_{12}(2.0\pm0.7)\times10^2$	$>10^5$	N/D	N/D
6	**F-Py**	pyridine-d5	$(1.83\pm0.03)\times10^4$	$K_{11}(5.5\pm0.3)\times10^4$ $K_{12}(2\pm1)\times10^3$	$K_{21}(1.9\pm0.1)\times10^3$ $K_{11}(9.0\pm0.1)\times10^3$	0.33	2.03
7	**F-Ph**	pyridine-d5	$(1.2\pm0.1)\times10^4$	$K_{11}(2.3\pm0.2)\times10^4$ $K_{12}(2.3\pm1.2)\times10^1$	$>10^5$	0.52	$\ll1$
8	**OPr-Py**	CD_2Cl_2/CD_3CN (1:3)	$(1.34\pm0.04)\times10^4$	$K_{11}(1.9\pm0.3)\times10^1$ $K_{12}(1.0\pm0.1)\times10^1$	<1	705	>13400
9	**OPr-Py**	pyridine-d5	$>10^5$	$K_{11}(7.8\pm0.7)\times10^2$ $K_{12}(1.8\pm0.1)\times10^1$	<1	>128	$>10^5$
10	**OPr-Ph**	CD_2Cl_2/CD_3CN (1:3)	$>10^5$	$(1.2\pm0.1)\times10^4$	$>10^5$	>8	N/D

[a] average of two runs; [b] assuming 1:1 stoichiometry; [c] Selectivity $S=K(A_1^-)/K(A_2^-)$. For experimental details, see Supporting Information.

concentrations an H_1G_1 complex ($K_{a(11)}(HSO_4^-)>10^5\ M^{-1}$) dominates.

From anion-π interaction studies it is known that the more electron-deficient the π-system is, the better is the anion stabilized.[12a,17i,28] Therefore, it is expected that the cages with electron-withdrawing bromide and fluoride substituents should enhance the affinity of the cages towards the planar nitrate anion. Due to the poor solubility, we could not perform the titration experiments of the halogenated cages in CD_2Cl_2/CD_3CN but had to switch to pyridine-d5. As the two solvent systems have different dielectric constants (pyridine $\varepsilon=12.4$, CH_2Cl_2/CH_3CN 1/3 $\varepsilon\sim30$) the obtained association constants in pyridine-d5 are expected to be substantially higher than in CD_2Cl_2/CD_3CN allowing no direct comparison. Therefore, we also performed NMR titrations with **Et-Py** in pyridine-d5 to obtain a rough conversion factor between the two solvent systems.[29] For **Et-Py** association constants of $K_{a(11)}(NO_3^-)=2.77\times10^3\ M^{-1}$ and $K_{a(12)}(NO_3^-)=6\times10^1\ M^{-1}$ for nitrate and $K_{a(11)}(Cl^-)=1.9\times10^3\ M^{-1}$ and $K_{a(12)}(Cl^-)=1.4\times10^2\ M^{-1}$ for chloride were determined, suggesting a factor of about 12–15 between the two solvents systems.

Indeed, as expected, with the more electron-poor substituents on the top and bottom rings, the association constants for **F-Py** increased about a factor of 6.5 to $K_a(NO_3^-)=1.78\times10^4\ M^{-1}$ in comparison to **Et-Py**. For **Br-Py** the binding was with $K_a(NO_3^-)=9.1\times10^3\ M^{-1}$ still three times higher than for **Et-Py**. For both pyridine-based cages **Br-Py** and **F-Py** also more chloride ($K_{a(11)}(Cl^-)=7\times10^3\ M^{-1}$, $K_{a(12)}(Cl^-)=4.8\times10^1\ M^{-1}$ and $K_{a(11)}(Cl^-)=5.5\times10^4\ M^{-1}$, $K_{a(12)}(Cl^-)=2\times10^3\ M^{-1}$) is bound than with the **Et-Py** cage and the selectivity for nitrate against chloride is decreased for both cages ($S_{Br\text{-}Py}$ (NO_3^-/Cl^-)=1.3 and $S_{F\text{-}Py}$ (NO_3^-/Cl^-)=0.33; Table 3). In contrast to **Et-Py**, **Br-Py** has very high association constants for hydrogensulfate ($K_{a(21)}(HSO_4^-)=7\times10^4\ M^{-1}$, $K_{a(11)}(HSO_4^-)=4.2\times10^3\ M^{-1}$), suggesting a H_2G_1-system to be preferred for **Br-Py**. For **F-Py** the same assumptions are made although $K_{a(21)}(HSO_4^-)=1.9\times10^3\ M^{-1}$, $K_{a(11)}(HSO_4^-)=9.0\times10^3\ M^{-1}$ are smaller than for **Br-Py**. Overall, the low selectivities of nitrate versus the other anions make these cages less good candidates for anion separation purposes.

Replacing pyridyl by phenyl in both cases gave diverging trends. Whereas **Br-Ph** binds nitrate much stronger ($K_a(NO_3^-)>10^5\ M^{-1}$) than **Br-Py**, for **F-Ph** it is in the same range ($K_a(NO_3^-)=1.2\times10^4\ M^{-1}$) as for **F-Py**. Similar as for the pair **Et-Py**/**Et-Ph**, **Br-Ph** had overall higher association constants for all anions than **Br-Py**. It is worth mentioning, that within the whole series, only for this host-guest couple NMR titration experiments showed two sets of signals for both $HSO_4^-\subset$**Br-Ph** and free **Br-Ph** (see Figure 2d), suggesting a slow exchange on the NMR time scale. There is only a marginal difference between **F-Ph** and **F-Py** in the anion recognition, with the exception that the phenyl-based cage is binding hydrogen sulfate with a very high K_a (HSO_4^-) $>10^5\ M^{-1}$), as all phenyl-based cages (see also below).

By replacing the ethyl substituents with n-propoxy groups, the affinities in pyridine-d5 were $K_a(NO_3^-)>10^5$, $K_{a(11)}(Cl^-)=7.8\times10^2\ M^{-1}$, $K_{a(12)}(Cl^-)=1.8\times10^1\ M^{-1}$ and $K_a(HSO_4^-)<1$ for **OPr-Py**, thus showing a remarkably good selectivity for nitrate, both over chloride and hydrogen sulfate ($S(NO_3^-/Cl^-)>128$ and $S(NO_3^-/HSO4^-)=10^5$). The association constant for nitrate exceeds the limit of measurability by ^{1}H NMR titration, so we switched back to the original and more polar solvent mixture CD_2Cl_2/CD_3CN (1:3) for the OPr-cages with affinities for nitrate of $K_a(NO_3^-)=1.34\times10^4\ M^{-1}$ for **OPr-Py** and even $K_a(NO_3^-)>10^5\ M^{-1}$ for **OPr-Ph**.

Some of the here described cages show the highest values reported for nitrate binding,[10a] however; some literature values are generated from different solvent systems and therefore it is difficult to compare.[29] In our opinion high affinities as sole criterium are not meaningful for potential applications. Instead, more important are selectivities rather than absolute numbers.

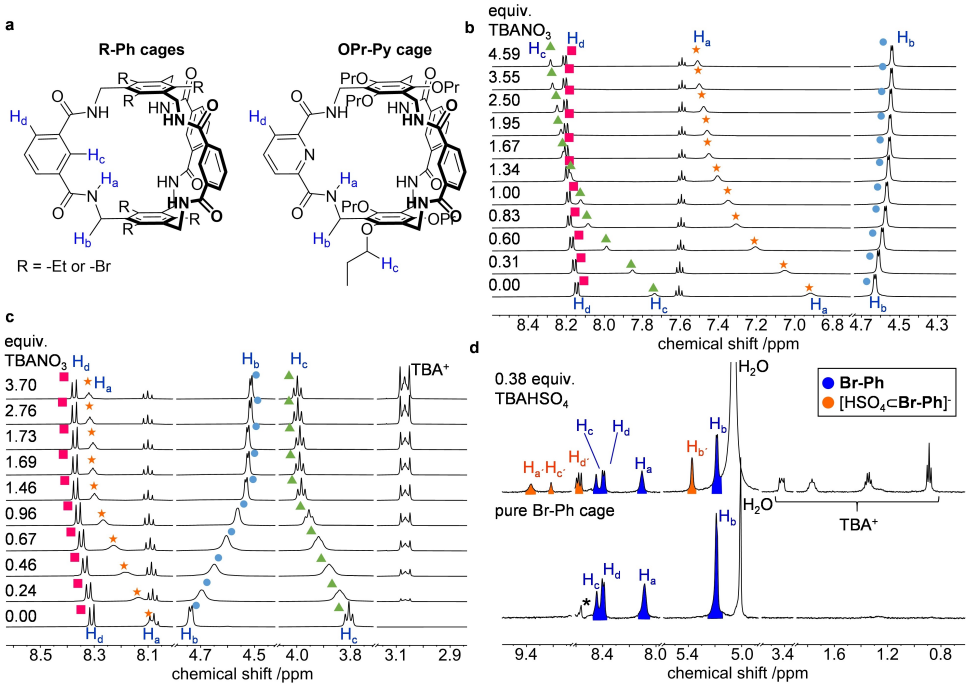

Figure 2. NMR titration experiments. a) assignment of protons; b) **Et-Ph** cage with NBu_4NO_3 in CD_2Cl_2/CD_3CN (1:3); c) **OPr-Py** cage with NBu_4NO_3 in CD_2Cl_2/CD_3CN (1:3); d) comparison of apohost **Br-Ph** and **Br-Ph** with NBu_4HSO_4 in pyridine-d5. All spectra were recorded at 500 MHz at room temp. For details, see Supporting Information.

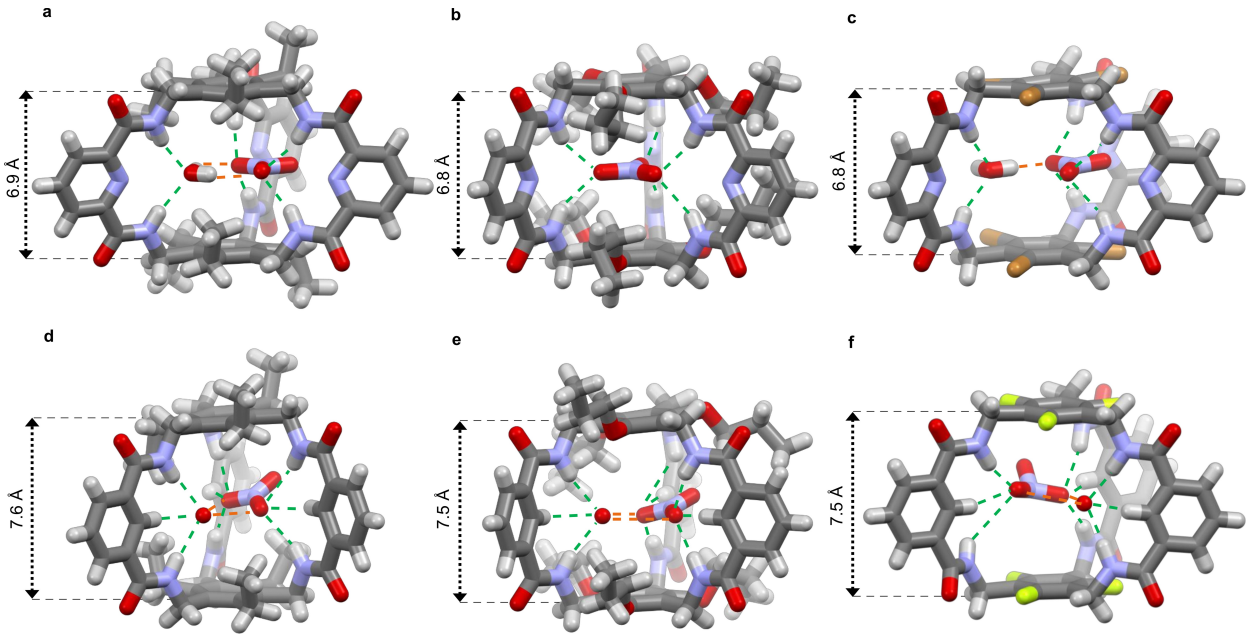

Figure 3. Crystal structure analysis of the nitrate complexes shown as capped sticks models. a) $NEt_4[NO_3⊂$**Et-Py**$]$, b) $NBu_4[NO_3⊂$**OPr-Py**$]$, c) $NBu_4[NO_3⊂$**Br-Py**$]$, d) $NBu_4[NO_3⊂$**Et-Ph**$]$, e) $NBu_4[NO_3⊂$**OPr-Ph**$]$, f) $NBu_4[NO_3⊂$**F-Ph**$]$. Hydrogen: white, carbon: grey, nitrogen: blue, oxygen: red, fluorine: green and bromine: orange. The distances between the π-planes of bottom and top benzene units are represented by double arrows. Hydrogen bonds between hosts and guests are displayed by dotted green lines, hydrogen bonds between two guests are displayed by dotted orange lines. Cations and solvate molecules are omitted for clarity. For more details, see Supporting Information.

Thus, the fact that, although **OPr-Py** binds less nitrate than **OPr-Ph**, it has a remarkable selectivity of $S_{OPr\text{-}Py}$ $(NO_3^-/Cl^-) = 705$ against chloride $(K_{a(11)}(Cl^-) = 1.9 \times 10^1\ M^{-1}$, $K_{a(12)}(Cl^-) = 1.0 \times 10^1\ M^{-1})$ as well as vs. hydrogen sulfate ($S_{OPr\text{-}Py}$ $(Cl^-/HSO_4^-) = 13400$; $K_a(HSO_4^-) < 1\ M^{-1}$). To the best of our knowledge, there is no system based on charge-neutral hosts reported with

comparable selectivities (see Table S3, Supporting Information). The best one is the macrocycle by Wang and coworkers with $S(NO_3^-/Cl^-) = 4.0$, determined in CD_3CN, a solvent with a comparable dielectric constant ($\varepsilon \sim 37$).[17i] **OPr-Ph** binds chloride ($K_a(Cl^-) = 1.2 \times 10^4\ M^{-1}$) better than **OPr-Py** and, similar as observed within the pair **Et-Py**/**Et-Ph** has a much higher affinity to hydrogensulfate K_a (HSO_4^-) $> 10^5\ M^{-1}$). Despite the higher binding constants, selectivities dropped to $S_{OPr\text{-}Ph}$ (NO_3^-/Cl^-) > 8.

Anslyn and co-workers described a number of crystal structures of host-guest complexes of **Et-Py** cage with various anions, but unfortunately the one with incorporated nitrate was missing.[14]

We were able to grow high-quality single crystals for six of the eight NO_3⊂cage complexes, which are depicted in Figure 3. All cages bind nitrate in a 1:1 stoichiometry and with the exception of **OPr-Py** (Figure 3b), in each other case one additional water molecule is found inside the cavity connecting the cages with the nitrate anions via hydrogen bonding. The average distance between the top and bottom aromatic unit is for pyridine based cages with 6.8–6.9 Å significantly smaller than for all phenyl-based cages (7.5–7.6 Å). This difference in distance explains the better fitting of nitrate to all pyridine-based cages being parallel sandwiched in between those aromatic units with an ideal distance for π-stacking.[30] In contrast, the space for efficient π-stacking is to large in all phenyl-based cages and indeed, here nitrate is not parallel oriented to the π-planes of the bottom and top aromatic rings, suggesting that these contributions play minor roles.[17h] For NO_3⊂**Et-Py** and NO_3⊂**Br-Py** the nitrate guest lies nearly parallel to the aromatic caps in the cage cavity, but is "pushed out" of the centre of the cage by the crystal water. For instance, in NO_3⊂**Et-Py** the incorporated water forms an intermolecular O–H···O–N hydrogen bond to the nitrate ($d = 2.26$ Å, Figure 3a, orange dotted lines) bridging the distance to the two remaining amide protons of the cage (N–H···O–H, $d = 2.19$ Å). In contrast, in NO_3⊂**OPr-Py** the nitrate anion is directly bound to all six amide hydrogen bonds ($d_{N\text{–}H\cdots O\text{–}N} = 2.33$–$2.65$ Å). The propoxy chains are all *endo*-oriented with a distance of their twelve α-protons to the nitrate anion of $d_{H\cdots O} = 2.8$–3.5 Å. This explains the observed downfield shift of the α-protons of **OPr-Py** during NMR-titration with NBu_4NO_3 (Figure 2c), suggesting that there is a certain contribution of the alkoxy protons to the binding of the guest, this preferred orientation of the propoxy chains is on one hand reducing the void space, which may cause a disadvantageous fit for hydrogensulfate and chloride, explaining the very high selectivities. Furthermore, the contact is stabilizing the host-guest complex NO_3⊂**OPr-Py** via dispersion interactions. For NBu_4[NO_3⊂**OPr-Ph**] we found a similar stabili-

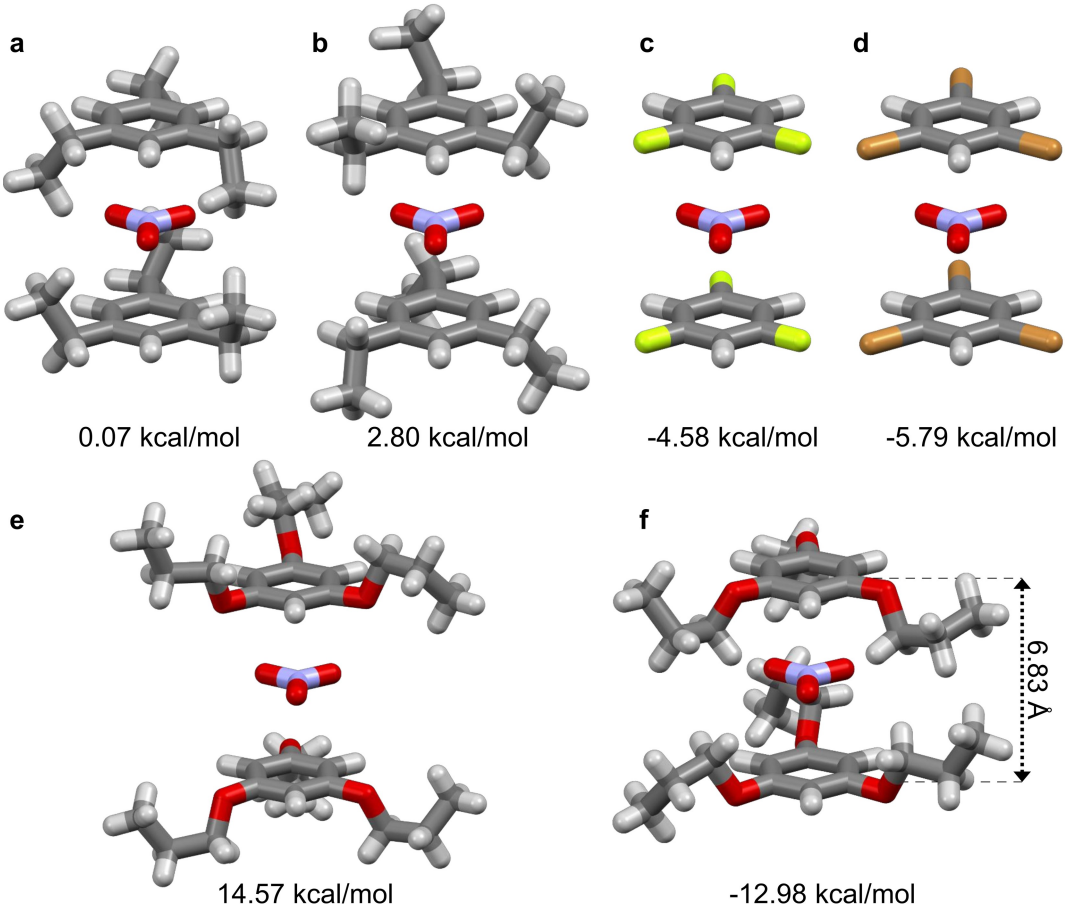

Figure 4. Calculated complexation energies (counterpoise Gaussian,[31] B3LYP aug-cc-pVDZ) in dependence on the substitution at the aromatic caps: a) ethyl in all down (*endo*) and b) all up (*exo*) conformation, c) fluoro, d) bromo, e) propoxy (*exo*), f) propoxy (*endo*) substitution.

zation of the nitrate guest via the propoxy-chains. Here only five of the six propoxy chains are oriented *endo*. The nitrate guest in the cavity of **F-Ph** is highly disordered, which makes it impossible to exactly determine hydrogen bond distances. The cavity is mainly filled with nitrate and water as co-guest. However, we found that the anion is also partially present without water, which could not be modelled completely. This "bad fit" may explain the comparable low association constant for nitrate.

The high affinity for nitrate found for **OPr-Py** in comparison to all other cages within this series is on first glance counter-intuitive, because n-propoxy substituents are more of electron donating nature than bromide or fluoride, which should result in lower affinities. To gain a deeper insight into the observed binding behavior, we have calculated the complexation energies of the nitrates with two aromatic rings (counterpoise Gaussian,[31] B3LYP aug-cc-pVDZ, Figure 4). To investigate only the influence of the substitution (–Et, –OPr, –F and –Br) on the π-surfaces, the linking bisamide units of the cages were deleted and the two aromatic fragments were placed at the exact distance from the nitrate that is observed from the crystal structure of $NBu_4[NO_3\subset$**OPr-Py**] (Figure 3b). As assumed and in agreement with the trends observed by NMR-titration the interaction energy of nitrate with the bromide- and fluoride substituted benzene rings is with −4.58 kcal/mol (F) and −5.78 kcal/mol (Br) significantly more stable than with the ethyl substituted cage. Again, in agreement with the NMR titration results, the energy difference between F– and Br– substitution is less pronounced than in comparison to ethyl or propoxy. For the two letter it makes a difference, whether the chains point outwards or towards the cage cavity. Whereas for ethyl this effect is relatively small [0.07 kcal/mol (*endo*) vs. 2.80 kcal/mol (exo)], it is very large for the propoxy substituted rings [−12.98 kcal/mol (*endo*) vs. +14.57 kcal/mol (*exo*)]. This result nicely fits to the observation made by X-ray crystallography as well as by NMR titrations that suggest that also in solution propoxy-chains point towards the cavity. Furthermore, this trend in complexation energy ($OPr_{endo} \gg Br > F > Et_{endo} > Et_{exo} \gg OPr_{exo}$), which follows the trend of our experimentally observed association constants of the Py-cages (OPr ≫ F ~ Br > Et).

We were also successful in obtaining single-crystal X-ray diffraction data for other host-guest complexes with anions different from nitrate. The solid state structure of the chloride complex $NBu_4[Cl\subset$**Br-Py**] was obtained by vapour diffusion with cyclohexane into a pyridine solution of **Br-Py** and NBu_4Cl (Figure 5a). The unit cell consists of one equivalent cyclohexane, four equivalents water and one equivalent NBu_4Cl per cage as well as two equivalents of water that are localized in the cavity and occupy the free space next to the chloride anion (N–H···O–H contacts, $d = 2.19$–2.31 Å). The anion is bound directly only to one of the three bridging amide wings of the cage via bifurcated N–H···Cl hydrogen bonds ($d = 2.47$–2.50 Å) and additionally stabilized by two water molecules via O–H···Cl hydrogen bonds ($d = 2.39$–2.41 Å). It is worth to be mentioned that in Anslyn's paper the **Et-Py** cage crystallized with two chloride anions bound.[14]

It turned out that despite high association constants for some of the amide cages with hydrogensulfate, it was rather difficult to get a single-crystal X-ray structure of those host-guest complexes. To our delight, we were able to obtain triclinic crystals of $NBu_4[HSO_4\subset$**F-Py**]. The complex crystallizes when hexane slowly diffused into a solution of **F-Py** and NBu_4HSO_4 in

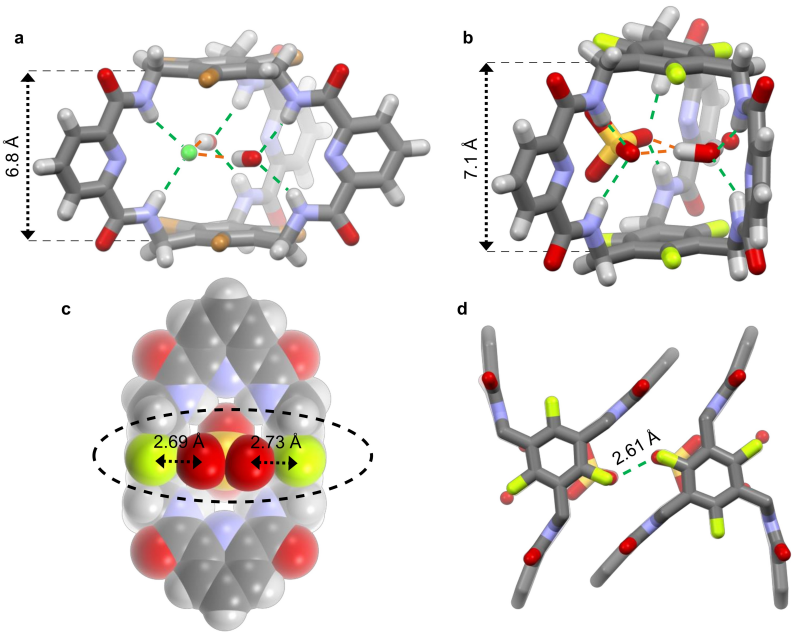

Figure 5. Crystal structure analysis of host guest complexes shown as capped sticks model. a) $NBu_4[Cl\subset$**Br-Py**]; b)-d) $NBu_4[HSO_4\subset$**F-Py**], The distances between the π-planes of bottom and top benzene units in a) and b) are represented by double arrows. Hydrogen bonds between hosts and guests are displayed by dotted green lines, hydrogen bonds between two guests are displayed by dotted orange lines. In c) the distances between F and O of the hydrogen sulfate are given. d) dimer formation. Cations and solvate molecules are omitted for clarity. For more details, see Supporting Information.

acetone (Figure 5b). The hydrogensulfate guest does not seem to fit completely into the cage cavity. The guest is bound by four of the six amide protons ($d_{N–H\cdots O–S}$ = 2.22–2.49 Å) in a bifurcated fashion and is additionally stabilized with a water molecule inside the cavity, which is itself connected via hydrogen bonds to the remaining wing.

The two outer oxygens of the hydrogensulfate are oriented such, that two C–F···O–S contacts with a distance (d = 2.69 Å and 2.73 Å) significantly smaller than the sum of the van-der-Waals radii (2.99 Å) are formed. The C–F bonds of the host and the S–O bonds are periplanar oriented with angles of C–F···O = 85.6° and 86.0° and S–O···F = 136.6° and 139.6°. In addition to that, two host-guest units form a dimer by interanionic hydrogen bonds[32] of the two adjacent HSO_4^--guests (Figure 5c and d).

Conclusion

To summarize, a series of [2 + 3] amide cages has been synthesized in a two-step approach by forming first the corresponding imine cages in high yields which were then converted in an improved Pinnick-oxidation protocol to the amide cages, again in very high yields. Overall yields up to > 90% were achieved by this method which is more than doubled in comparison to prior one-step approaches by using 'classical' amide bond formation reactions of acid chloride units with amines (40%).

The eight structurally slightly varying amide cages were investigated as hosts for anion binding in search for a selective nitrate complexation. Although some of the cages (e.g., **Br-Ph** or **OPr-Ph**) showed very high affinities towards nitrate with $K_a > 10^5\ M^{-1}$ we were more delighted by the superior selectivity of **OPr-Py** for nitrate vs. chloride (S = 705) or hydrogensulfate (S > 13400) although the nitrate binding constant was a bit lower [$K_a(NO_3^-) = 13.4 \times 10^4\ M^{-1}$]. To the best of our knowledge, this high selectivity is unprecedented and can be explained by the propoxy-chains pointing towards the cavity, contributing to interacting with the nitrate anion as well as reducing the cavities volume. This assumption has been supported by calculations, NMR investigations as well as by single-crystal structure analysis of all host-guest complexes with nitrate.

This 2nd generation of [2 + 3] amide cage host compound will now be taken as lead structure to further increase selectivity of anion recognition, to create high sensible sensors or porous materials to remove nitrate from drinking water.

Deposition Number(s) 2154545 (1,3,5-tris(bromomethyl)-2,4,6-tripropoxybenzol), 2154550 (**4**), 2154563 (**4**), 2154553 (NEt_4[NO_3@**4**]), 2154546 (**12**), 2154562 (**14**), 2154552 (NBu_4[NO_3@**14**]), 2154549 (**15**), 2154551 (NBu_4[NO_3@**15**]), 2154547 (**16**), 2154561 (**16**), 2154554 (NBu_4[NO_3@**16**]), 2154557 (**17**), 2154560 (NBu_4[NO_3@**18**]), 2154548 (**19**), 2154555 (NBu_4[NO_3@**19**]), 2154556 (NBu_4[Cl@**19**]), 2154558 (**20**) contain(s) the supplementary crystallographic data for this paper. These data are provided free of charge by the joint Cambridge Crystallographic Data Centre and Fachinformationszentrum Karlsruhe Access Structures service.

Acknowledgements

We thank the European Research Council ERC in the frame of the consolidators grant CaTs n DOCs (grant no. 725765) and Deutsche Forschungsgemeinschaft DFG under Germany's Excellence Strategy Cluster 3D Matter Made to Order (EXC-2082/1 – 390761711) for funding this project. Open Access funding enabled and organized by Projekt DEAL.

Conflict of Interest

The authors declare no conflict of interest.

Data Availability Statement

The data that support the findings of this study are available from the corresponding author upon reasonable request.

Keywords: amides · anions · dynamic covalent chemistry · noncovalent interactions · organic cage compounds

[1] G. Zhang, M. Mastalerz, *Chem. Soc. Rev.* **2014**, *43*, 1934–1947.
[2] M. Mastalerz, *Acc. Chem. Res.* **2018**, *51*, 2411–2422.
[3] a) M. A. Little, A. I. Cooper, *Adv. Funct. Mater.* **2020**, *30*, 1909842; b) F. Beuerle, B. Gole, *Angew. Chem. Int. Ed.* **2018**, *57*, 4850–4878; *Angew. Chem.* **2018**, *130*, 4942–4972; c) M. Liu, L. Zhang, M. A. Little, V. Kapil, M. Ceriotti, S. Yang, L. Ding, D. L. Holden, R. Balderas-Xicohténcatl, D. He, R. Clowes, S. Y. Chong, G. Schütz, L. Chen, M. Hirscher, A. I. Cooper, *Science* **2019**, *366*, 613–620; d) T. Hasell, M. Miklitz, A. Stephenson, M. A. Little, S. Y. Chong, R. Clowes, L. Chen, D. Holden, G. A. Tribello, K. E. Jelfs, A. I. Cooper, *J. Am. Chem. Soc.* **2016**, *138*, 1653–1659; e) T. Mitra, K. E. Jelfs, M. Schmidtmann, A. Ahmed, S. Y. Chong, D. J. Adams, A. I. Cooper, *Nat. Chem.* **2013**, *5*, 276; f) S. M. Elbert, F. Rominger, M. Mastalerz, *Chem. Eur. J.* **2014**, *20*, 16707–16720; g) G. Zhang, O. Presly, F. White, I. M. Oppel, M. Mastalerz, *Angew. Chem. Int. Ed.* **2014**, *53*, 1516–1520; *Angew. Chem.* **2014**, *126*, 1542–1546; h) S. M. Elbert, N. I. Regenauer, D. Schindler, W.-S. Zhang, F. Rominger, R. R. Schröder, M. Mastalerz, *Chem. Eur. J.* **2018**, *24*, 11438–11443; i) T. Jiao, L. Chen, D. Yang, X. Li, G. Wu, P. Zeng, A. Zhou, Q. Yin, Y. Pan, B. Wu, X. Hong, X. Kong, V. M. Lynch, J. L. Sessler, H. Li, *Angew. Chem. Int. Ed.* **2017**, *56*, 14545–14550; *Angew. Chem.* **2017**, *129*, 14737–14742.
[4] a) A. Kewley, A. Stephenson, L. J. Chen, M. E. Briggs, T. Hasell, A. I. Cooper, *Chem. Mater.* **2015**, *27*, 3207–3210; b) J. H. Zhang, S. M. Xie, L. Chen, B. J. Wang, P. G. He, L. M. Yuan, *Anal. Chem.* **2015**, *87*, 7817–7824; c) Y. Wang, H. X. Li, S. M. Xie, B. J. Wang, J. H. Zhang, L. M. Yuan, *Microchem. J.* **2021**, *170*.
[5] a) M. Brutschy, M. W. Schneider, M. Mastalerz, S. R. Waldvogel, *Adv. Mater.* **2012**, *24*, 6049–6052; b) M. Brutschy, M. W. Schneider, M. Mastalerz, S. R. Waldvogel, *Chem. Commun.* **2013**, *49*, 8398–8400.
[6] a) J. C. Lauer, Z. Pang, P. Janßen, F. Rominger, T. Kirschbaum, M. Elstner, M. Mastalerz, *Chem. Open* **2020**, *9*, 183–190; b) K. Acharyya, P. S. Mukherjee, *Chem. Commun.* **2014**, *50*, 15788–15791; c) N. Nishimura, K. Yoza, K. Kobayashi, *J. Am. Chem. Soc.* **2010**, *132*, 777–790; d) O. Shyshov, R.-C. Brachvogel, T. Bachmann, R. Srikantharajah, D. Segets, F. Hampel, R. Puchta, M. von Delius, *Angew. Chem. Int. Ed.* **2017**, *56*, 776–781; *Angew. Chem.* **2017**, *129*, 794–799.
[7] a) N. Busschaert, C. Caltagirone, W. Van Rossom, P. A. Gale, *Chem. Rev.* **2015**, *115*, 8038–8155; b) M. J. Langton, C. J. Serpell, P. D. Beer, *Angew. Chem. Int. Ed.* **2016**, *55*, 1974–1987; *Angew. Chem.* **2016**, *128*, 2012–2026; c) P. Molina, F. Zapata, A. Caballero, *Chem. Rev.* **2017**, *117*, 9907–9972; d) X. Wu, A. M. Gilchrist, P. A. Gale, *Chem* **2020**, *6*, 1296–1309; e) L. Chen, S. N. Berry, X. Wu, E. N. W. Howe, P. A. Gale, *Chem* **2020**, *6*, 61–141; f) N. H. Evans, P. D. Beer, *Angew. Chem. Int. Ed.* **2014**, *53*, 11716–11754; *Angew. Chem.* **2014**, *126*, 11908–11948; g) S. O. Kang, R. A. Begum, K. Bowman-James, *Angew. Chem. Int. Ed.* **2006**, *45*, 7882–7894;

Angew. Chem. **2006**, *118*, 8048–8061; h) D.-X. Wang, M.-X. Wang, *Acc. Chem. Res.* **2020**, *53*, 1364–1380.
[8] S. O. Kang, J. M. Llinares, V. W. Day, K. Bowman-James, *Chem. Soc. Rev.* **2010**, *39*, 3980–4003.
[9] Y. Liu, W. Zhao, C.-H. Chen, A. H. Flood, *Science* **2019**, *365*, 159–161.
[10] a) H. Xie, T. J. Finnegan, V. W. Liyana Gunawardana, R. Z. Pavlović, C. E. Moore, J. D. Badjić, *J. Am. Chem. Soc.* **2021**, *143*, 3874–3880; b) H. Xie, V. W. L. Gunawardana, T. J. Finnegan, W. Xie, J. D. Badjic, *Angew. Chem. Int. Ed. Engl.* **2022**, *61*, e202116518.
[11] a) D.-H. Tuo, Y.-F. Ao, Q.-Q. Wang, D.-X. Wang, *Org. Lett.* **2019**, *21*, 7158–7162; b) S. I. Etkind, D. A. Vander Griend, T. M. Swager, *J. Org. Chem.* **2020**, *85*, 10050–10061; c) J. Luo, J. Zhu, D.-H. Tuo, Q. Yuan, L. Wang, X.-B. Wang, Y.-F. Ao, Q.-Q. Wang, D.-X. Wang, *Chem. Eur. J.* **2019**, *25*, 13275–13279.
[12] a) N. Luo, Y.-F. Ao, D.-X. Wang, Q.-Q. Wang, *Angew. Chem. Int. Ed.* **2021**, *60*, 20650–20655; b) N. Luo, Y.-F. Ao, D.-X. Wang, Q.-Q. Wang, *Chem. Asian J.* **2021**, *16*, 3599–3603.
[13] a) K. Bowman-James, *Acc. Chem. Res.* **2005**, *38*, 671–678; b) S. O. Kang, J. M. Llinares, D. Powell, D. VanderVelde, K. Bowman-James, *J. Am. Chem. Soc.* **2003**, *125*, 10152–10153.
[14] A. P. Bisson, V. M. Lynch, M.-K. C. Monahan, E. V. Anslyn, *Angew. Chem. Int. Ed.* **1997**, *36*, 2340–2342; *Angew. Chem.* **1997**, *109*, 2435–2437.
[15] a) V. H. Smith, D. W. Schindler, *Trends Ecol. Evol.* **2009**, *24*, 201–207; b) R. F. Follett, J. L. Hatfield, *Sci. World J.* **2001**, *1 Suppl. 2*, 920–926.
[16] M. H. Ward, R. R. Jones, J. D. Brender, T. M. de Kok, P. J. Weyer, B. T. Nolan, C. M. Villanueva, S. G. van Breda, *Int. J. Environ. Res. Public Health* **2018**, *15*.
[17] a) R. Dutta, P. Ghosh, *Chem. Commun.* **2015**, *51*, 9070–9084; b) T. A. Barendt, A. Docker, I. Marques, V. Félix, P. D. Beer, *Angew. Chem. Int. Ed.* **2016**, *55*, 11069–11076; *Angew. Chem.* **2016**, *128*, 11235–11242; c) K. Choi, A. D. Hamilton, *J. Am. Chem. Soc.* **2001**, *123*, 2456–2457; d) R. Herges, A. Dikmans, U. Jana, F. Köhler, P. G. Jones, I. Dix, T. Fricke, B. König, *Eur. J. Org. Chem.* **2002**, *2002*, 3004–3014; e) P. Blondeau, J. Benet-Buchholz, J. de Mendoza, *New J. Chem.* **2007**, *31*, 736–740; f) A. S. Singh, S.-S. Sun, *J. Org. Chem.* **2012**, *77*, 1880–1890; g) J. Romański, P. Piątek, *J. Org. Chem.* **2013**, *78*, 4341–4347; h) M. M. Watt, L. N. Zakharov, M. M. Haley, D. W. Johnson, *Angew. Chem. Int. Ed.* **2013**, *52*, 10275–10280; *Angew. Chem.* **2013**, *125*, 10465–10470; i) D.-X. Wang, M.-X. Wang, *J. Am. Chem. Soc.* **2013**, *135*, 892–897; j) S. Chakraborty, R. Dutta, B. M. Wong, P. Ghosh, *RSC Adv.* **2014**, *4*, 62689–62693; k) A. Tasada, F. M. Albertí, A. Bauzá, M. Barceló-Oliver, A. García-Raso, J. J. Fiol, E. Molins, A. Caubet, A. Frontera, *Chem. Commun.* **2013**, *49*, 4944–4946.
[18] J. W. Steed, J. L. Atwood, in *Supramolecular Chemistry*, 2nd ed., Wiley, **2009**, pp. 223–284.
[19] a) D. A. Leigh, P. J. Lusby, A. M. Z. Slawin, D. B. Walker, *Angew. Chem. Int. Ed.* **2005**, *44*, 4557–4564; *Angew. Chem.* **2005**, *117*, 4633–4640; b) D. A. Leigh, P. J. Lusby, A. M. Z. Slawin, D. B. Walker, *Chem. Commun.* **2005**, 4919–4921; c) A. M. L. Fuller, D. A. Leigh, P. J. Lusby, *J. Am. Chem. Soc.* **2010**, *132*, 4954–4959.
[20] T. S. Snowden, A. P. Bisson, E. V. Anslyn, *J. Am. Chem. Soc.* **1999**, *121*, 6324–6325.
[21] A. S. Bhat, S. M. Elbert, W.-S. Zhang, F. Rominger, M. Dieckmann, R. R. Schröder, M. Mastalerz, *Angew. Chem. Int. Ed.* **2019**, *58*, 8819–8823; *Angew. Chem.* **2019**, *131*, 8911–8915.
[22] a) M. Arunachalam, I. Ravikumar, P. Ghosh, *J. Org. Chem.* **2008**, *73*, 9144–9147; b) P. Mateus, R. Delgado, P. Brandão, S. Carvalho, V. Félix, *Org. Biomol. Chem.* **2009**, *7*, 4661–4673; c) N. De Rycke, J. Marrot, F. Couty, O. R. P. David, *Tetrahedron Lett.* **2010**, *51*, 6521–6525; d) T. H. G. Schick, F. Rominger, M. Mastalerz, *J. Org. Chem.* **2020**, *85*, 13757–13771; e) T. H. G. Schick, J. C. Lauer, F. Rominger, M. Mastalerz, *Angew. Chem. Int. Ed.* **2019**, *58*, 1768–1773; *Angew. Chem.* **2019**, *131*, 1782–1787.
[23] a) B. O. Lindgren, T. Nilsson, *Acta Chem. Scand.* **1973**, *27*, 888–890; b) B. S. Bal, W. E. Childers, H. W. Pinnick, *Tetrahedron* **1981**, *37*, 2091–2096; c) E. Dalcanale, F. Montanari, *J. Org. Chem.* **1986**, *51*, 567–569; d) M. A. Mohamed, K. Yamada, K. Tomioka, *Tetrahedron Lett.* **2009**, *50*, 3436–3438.
[24] A. A. Hussein, A. A. M. Al-Hadedi, A. J. Mahrath, G. A. I. Moustafa, F. A. Almalki, A. Alqahtani, S. Shityakov, M. E. Algazally, *Roy. Soc. Open Sci.* **2020**, *7*.
[25] a) X. Y. Hu, W. S. Zhang, F. Rominger, I. Wacker, R. R. Schroder, M. Mastalerz, *Chem. Commun.* **2017**, *53*, 8616–8619; b) M. Holsten, S. Feierabend, S. M. Elbert, F. Rominger, T. Oeser, M. Mastalerz, *Chem. Eur. J.* **2021**, *27*, 9383–9390.
[26] P.-E. Alexandre, W.-S. Zhang, F. Rominger, S. M. Elbert, R. R. Schröder, M. Mastalerz, *Angew. Chem. Int. Ed.* **2020**, *59*, 19675–19679; *Angew. Chem.* **2020**, *132*, 19843–19847.
[27] F. Ulatowski, K. Dabrowa, T. Balakier, J. Jurczak, *J. Org. Chem.* **2016**, *81*, 1746–1756.
[28] Y. Zhao, C. Beuchat, Y. Domoto, J. Gajewy, A. Wilson, J. Mareda, N. Sakai, S. Matile, *J. Am. Chem. Soc.* **2014**, *136*, 2101–2111.
[29] a) Y. Liu, A. Sengupta, K. Raghavachari, A. H. Flood, *Chem* **2017**, *3*, 411–427; b) T. J. Sherbow, H. A. Fargher, M. M. Haley, M. D. Pluth, D. W. Johnson, *J. Org. Chem.* **2020**, *85*, 12367–12373.
[30] R. Thakuria, N. K. Nath, B. K. Saha, *Cryst. Growth Des.* **2019**, *19*, 523–528.
[31] a) S. F. Boys, F. Bernardi, *Mol. Phys.* **1970**, *19*, 553–566; b) S. Simon, M. Duran, J. J. Dannenberg, *J. Chem. Phys.* **1996**, *105*, 11024–11031.
[32] W. Zhao, A. H. Flood, N. G. White, *Chem. Soc. Rev.* **2020**, *49*, 7893–7906.

Manuscript received: May 17, 2022
Accepted manuscript online: June 14, 2022
Version of record online: July 21, 2022